JMBFS

Journal of Microbiology, Biotechnology and Food Sciences

International peer-reviewed scientific online journal

Published by Faculty of Biotechnology and Food Sciences

EVALUATING THE BIOLOGICAL ACTIVITIES OF SILVER AND ZINC OXIDE NANOPARTICLES BIOSYNTHESIZED BY *NEOWESTIELLOPSIS PERSICA* A1387

Omid Sabzevari Joopari[1], *Amir Eghbal Khajerahimi* *[2], *Reza Kazempoor**[3], *Bahareh Nowruzi*[4]

Address(es):
[1] Department of Aquatic Animal Health and Diseases, Science and Research Branch, Islamic Azad University, Tehran, Iran.
[2*]Department of Marine Science and Technology, Islamic Azad University, North Tehran Branch, North Tehran, Iran.
[3*]Department of Biology, Roudehen Branch, Islamic Azad University, Roudehen, Iran.
[4]Department of Biotechnology, Faculty of Converging Sciences and Technologies, Islamic Azad University, Science and Research Branch, Tehran, Iran.

*Corresponding author: Khajerahimi@srbiau.ac.ir, r.kazempoor@riau.ac.ir

https://doi.org/10.55251/jmbfs.10397

ARTICLE INFO

Received 24. 7. 2023
Revised 15. 10. 2024
Accepted 16. 10. 2024
Published xx.xx.201x

Regular article

OPEN ACCESS

ABSTRACT

In this research, the antimicrobial properties of zinc oxide (ZnO NPs) and silver (AgNPs) nanoparticles, synthesized biologically using Neowestiellopsis persica through various methods (such as wet biomass, boiling biomass, supernatant, extracellular polysaccharides, and phycocyanin), were examined against fish pathogens including Aeromonas hydrophila, Edwardsiella tarda, Yersinia enterocolitica, and Pseudomonas putida. The nanoparticles were successfully created using all methods and characterized employing techniques like UV-visible spectroscopy, scanning electron microscopy (SEM), Fourier transform infrared spectroscopy (FTIR), and dynamic light scattering (DLS). The antibacterial activity of the nanoparticles was assessed using agar-well diffusion assays, while transmission electron microscopy (TEM) was utilized to analyze the ultrastructural interactions between the nanoparticles and the pathogens. Cytotoxicity was evaluated via the trypan blue exclusion method. Notably, nanoparticles generated through the boiling-biomass method demonstrated significantly enhanced characteristics. The analysis revealed two distinct populations of AgNPs measuring 78.82 nm (41.2%) and 91.28 nm (45.5%), along with a pronounced absorption peak at 68.6 nm (80.1%) for ZnO NPs. AgNPs exhibited the strongest growth inhibition against Pseudomonas putida and Edwardsiella tarda, whereas ZnO NPs showed the largest inhibition zone against Yersinia enterocolitica, Pseudomonas aeruginosa, and Aeromonas hydrophila. TEM imagery illustrated the binding of nanoparticles to the outer membranes of Yersinia enterocolitica, compromising their structural integrity. The application of 25 µg/ml of AgNPs and 6.25 µg/ml of ZnO did not lead to significant cell death, but higher concentrations resulted in a dose-dependent cytotoxic effect. Ultimately, the findings of this study confirm that the antibacterial and cytotoxic attributes of silver and zinc oxide nanoparticles, produced through the biosynthesis of Neowestiellopsis persica A1387, can be leveraged to meet future needs in aquaculture.

Keywords: *Neowestiellopsis persica*, Cyanobacteria, Fish pathogens, silver nanoparticle, zinc oxide nanoparticle

INTRODUCTION

In contemporary times, with the burgeoning global population, food security stands as one of the most pressing challenges confronting human societies, and it is anticipated that the demand for fish and fish products will rise, given their status as the most affordable and readily available source of animal protein in comparison to other protein sources. Moreover, numerous studies have demonstrated that consuming fish diminishes the risk of mortality from cardiovascular diseases **(Chen et al., 2022; Krešić et al., 2022)**.
Similar to other animals, fish are susceptible to a range of diseases, including infections caused by pathogens, which are particularly prevalent in young fish with a compromised immune system **(Soror et al., 2022)**. To prevent and combat numerous diseases, a diverse array of chemicals, such as hormones, vitamins, antibiotics, and other substances, have been evaluated for various treatments in aquaculture practices. These compounds encompass synthetic disinfectants (hydrogen peroxide and malachite green), antibiotics (sulfonamides and tetracycline), anthelmintic agents, and natural substances like probiotics, essential oils, and herbal remedies **(Testerman et al., 2022)**. In numerous instances, pathogens exhibit resistance to these factors, and despite their beneficial effects, they should not be routinely prescribed owing to their potential adverse effects on both fish and humans. The continual use of antibiotics can result in the emergence of drug-resistant strains that can be transmitted to humans **(Zhang et al., 2022)**. Studies have indicated that tetracycline is the most commonly employed antibiotic in fish farms, and there exists a robust association between the emergence of antibiotic-resistant bacteria and the excessive use of antibiotics in aquaculture. Another study revealed that certain species of Aeromonas hydrophlia isolated from tilapia fish demonstrated resistance to broad-spectrum antibiotics such as tetracycline, streptomycin, and erythromycin. Antibiotic resistance has also been documented in Aeromonas salmonicida, Photobacterium damselae, Yersinia ruckeri, Vibrio sp., Listeria sp., Pseudomonas sp., and Edwardsiella sp. **(Okeke et al., 2022; Peng et al., 2022)**. Furthermore, researchers isolated antibiotic-resistant enterococcus from fish farms and postulated that these resistant bacteria in fish could transmit the infection to humans **(Sivaraman et al., 2022)**. Food safety is a paramount concern for both food industries and consumers, and due to the escalating prevalence of foodborne illnesses globally, an alternative solution is imperative to address the challenges confronting food businesses **(Adeyemi et al., 2022)**.
Over the last several decades, in the realm of developing antimicrobial agents with minimal adverse effects, metallic nanoparticles, due to their physical, chemical, and biological properties, have garnered significant interest. Contemporary research has demonstrated that meticulously engineered metallic nanoparticles possess satisfactory antibacterial efficacy, and antimicrobial formulations incorporating these agents can be potent antibacterial substances. Metallic oxides, beyond their antibacterial capabilities, offer an additional benefit by delivering crucial mineral elements to host cells **(Ifijen et al., 2022)**. Silver is among the metallic antimicrobial agents and has been extensively employed since antiquity to combat infections and manage pollution. The antimicrobial and antiviral properties of silver, zinc, and their corresponding compounds have been comprehensively examined **(Franco et al., 2022)**. Inorganic nanoparticles have exhibited innovative and improved biological functions attributed to their dimensions and configuration, and can be easily and affordably synthesized and manufactured in large quantities **(Tsikourkitoudi et al., 2022)**. While microbial-derived nanoparticles find widespread applications in biomedicine, healthcare, medical diagnostics **(Anvar et al., 2022; Nowruzi, 2022)**, and other domains, contemporary understanding acknowledges that a significant portion of these nanoparticles can pose risks to both human and aquatic life **(Mathew and Radhakrishnan, 2022)**. Nevertheless, cyanobacteria, being non-pathogenic organisms, have captivated the interest of numerous researchers in the biosynthesis of nanoparticles with minimal adverse effects on humans and animals. Owing to their capacity to sequester heavy metals from their surroundings, cyanobacteria stand out as one of the most valuable natural contenders employed in the biosynthesis of nanoparticles **(Chan et al., 2022; Golizadeh et al., 2022)**. Additionally, they harbor a diverse array of bioactive compounds, such as pigments

and enzymes, which can potentially function as reducing and stabilizing agents **(Anvar et al., 2021; Mutoti et al., 2022)**.

Literature has documented the antibacterial, antifungal, anti-algal, anticancer, and photocatalytic properties of nanoparticles synthesized by cyanobacteria **(El Semary and Bakir, 2022)**. Furthermore, studies have explored the cyanobacteria-mediated biosynthesis of metallic nanoparticles **(Fritz et al., 2022)**, yet the diverse synthesis methodologies that exert substantial influences on the final product characteristics often remain under-discussed. Empirical evidence has established that the nanoparticle synthesis method significantly impacts their various attributes, including size, shape, antimicrobial capabilities, cytotoxicity, and more **(Hamida et al., 2020)**.

The genus Neowestiellopsis was initially characterized by **Kabirnataj et al. (Kabirnataj et al., 2018)** from Mazandaran (Iran). This microorganism is classified within the Nostocales order and the Hapalosiphonaceae family **(Guiry and Guiry, 2020)**. Strains of this genus can be identified in both rice paddies and agricultural regions, and owing to their nitrogen-fixing capabilities, certain strains play a crucial role in agriculture **(Ahmadi and Nourouzi, 2008; Jochum et al., 2018)**. Numerous studies within the existing literature highlight the diverse biomedical applications of zinc and silver nanoparticles in aquaculture **(Golizadeh et al., 2022; Sabzevari et al., 2022)**. Despite the need for further investigations into the antimicrobial efficacy of these agents against fish pathogens **(Tsikourkitoudi et al., 2022)**. Given this context, examining the antipathogenic activity and cytotoxicity of nanoparticles biologically synthesized by Iranian cyanobacterial strains, in conjunction with comparing their various synthesis methods, could be instrumental in integrating these valuable organisms into the medical and pharmaceutical sectors.

MATERIAL AND METHODS

Cultivation of *Neowestiellopsis persica A1387*

Neowestiellopsis persica A1387 (*Hapalosiphonaceae*) was acquired from the Cyanobacteria Culture Collection (CCC) and Alborz herbarium at the Science and Research Branch, Islamic Azad University, Tehran, with the accession number A1387. Purified cultures were cultivated in BG11 medium at a temperature of 28±2ºC with intermittent agitation (twice daily). The culture chamber was illuminated with approximately 50-55 µmol photons m-2s-1 under a photoperiod of 14:10 hours of light-dark cycling **(Liu et al., 2014)**.

Silver and zinc oxide nanoparticles synthesis

The biosynthesis of silver (AgNPs) and zinc oxide (ZnO NPs) nanoparticles was conducted through five distinct methodologies, employing silver nitrate and zinc acetate as the silver and zinc precursors, respectively.

Biosynthesis of nanoparticles using wet biomass method

Subsequent to the logarithmic phase as described by **Cepoi et al. (Cepoi et al., 2015)**, the cultures were separated through centrifugation at 5000 rpm for 10 minutes at 20°C, followed by three washing cycles with distilled water. Subsequently, wet biomass (1 gram) was introduced into a 500 ml flask containing 100 ml of silver nitrate or zinc acetate solution at varying concentrations (1, 2, and 3 mM) (pH = 7), and the mixture was stored at 25 °C for a duration of 24 hours.

Biosynthesis of nanoparticles using supernatant method

In this approach, following the methodology outlined by **Patel et al. (2015)**, logarithmic phase cultures were centrifuged at 5000 rpm for 5 minutes, and the resulting supernatant (10, 20, and 30%) was incorporated into a 1 mM silver nitrate or zinc acetate solution at varying concentrations (1, 2, and 3 mM). The inoculated mixtures were subjected to continuous agitation at a temperature of 28-30 °C, and sampling was conducted at various time intervals (0, 12, 24, 48, and 72 hours). Every 12 hours, one milliliter of the liquid solution was collected, centrifuged at 5000 rpm for 5 minutes, and subsequently analyzed using spectrometry with a resolution of 1 nm within the wavelength range of 300 to 800 nm. Spectral peaks within the range of 420 to 500 nm were interpreted as indicative of silver nanoparticles, while the peak around 380 nm was associated with zinc oxide nanoparticles.

Biosynthesis of nanoparticles using boiling the biomass method

Cyanobacterial cultures were subjected to centrifugation at 2500 rpm for duration of ten minutes to isolate biomass, as previously documented **(Golizadeh et al., 2022)**. Subsequently, the biomass was desiccated in an oven at a temperature of 60 °C. One gram of desiccated biomass was subjected to boiling in 10 ml of distilled water for 15 minutes at 100 °C within an Erlenmeyer flask. Subsequent to boiling, the resulting mixture was cooled and centrifuged at 10,000 rpm for 15 minutes, followed by the collection and storage of the supernatant at 4 °C. Cell-free extracts of cyanobacterial strains were utilized for the synthesis of nanoparticles. Two milliliters of the extract were introduced into 10 ml of 1 mM silver nitrate or zinc acetate solution within 100 ml Erlenmeyer flasks. The reaction mixture was maintained at a temperature of 100 °C with continuous agitation. The initially colorless solution gradually transitioned to a yellowish-brown hue and subsequently to a darker brown shade after 45 minutes. The color alteration was observed, and the formation of nanoparticles was quantified through spectrometry. The synthesized nanoparticles were isolated through centrifugation at 15000 rpm for 20 minutes at 4 °C. The resulting pellet was subjected to multiple washing cycles with distilled water, followed by the use of 90% ethanol to eliminate impurities, ultimately yielding pure nanoparticle powder.

Biosynthesis of nanoparticles using phycocyanin pigments

To isolate phycocyanin, 500 ml of the 14-day culture medium was subjected to centrifugation at 4000 rpm, and the resulting precipitate was washed with phosphate buffer (pH: 7.2) and lyophilized. Two grams of freeze-dried biomass were dispersed in 500 ml of sodium phosphate buffer (0.1 M, pH 7.2). Phycobiliproteins were extracted through a process involving freezing at -20 °C and subsequent thawing at room temperature in a dark environment. The resulting mixture was centrifuged at 5,000 rpm for 30 minutes at 5 °C, and the phycoerythrin content was isolated and frozen. The purity of the pigment was assessed using the ratio of OD 620/OD 280. The biosynthesis of nanoparticles entailed dissolving the pigments (5 mg/ml) in 10 ml of a liquid solution containing 1 mM silver nitrate or zinc acetate. Subsequently, the resulting mixture was exposed to fluorescent light at 25 °C, and spectrometry was conducted at 12-hour intervals **(Ranjitha et al., 2020)**.

Biosynthesis of nanoparticles using extracellular polysaccharides

The biomass of the strain during the logarithmic phase was isolated through centrifugation at 3000 rpm, and the supernatant was utilized to extract the extracellular polysaccharides. Subsequently, ethanol (95%, v/v 1:1) was incorporated into the supernatant, and the mixture was stored at -20°C overnight. Precipitated polysaccharides were isolated through centrifugation at 10000 rpm, and following freeze-drying, their total weight was determined. Subsequently, 1.3 mg/ml of dried polysaccharide was dispersed in 3 ml of 1 mM silver nitrate or zinc acetate solution (pH: 7), and the mixture was then divided into two test tubes. The tubes were incubated at 25 °C under fluorescent light, and the absorbance spectra were analyzed at 12-hour intervals **(Patel et al., 2015)**.

UV-Vis Spectrophotometry

The absorption spectra of the nanoparticles were characterized using a UV-3600 plus UV-Vis-NIR spectrophotometer (Shimadzu, Japan), with the spectrum of deionized water serving as a reference (Figs. 1 and 2). All measurements were conducted at 25 °C over three distinct days. The wavelength range spanned from 300 to 600 nm, comparing against a blank (sterile BG11 broth).

Characterization of silver and zinc oxide nanoparticles

Dynamic Light Scattering (DLS) and zeta potential

Nanoparticle size and size distribution were estimated using dynamic light scattering (DLS) with the Zetasizer Nano ZS, Malvern Instrument, at a scattering angle of 90º under ambient conditions. The DLS analysis was conducted in triplicate on diluted nanoparticle suspensions in deionized distilled water. The absorption spectra of the nanoparticles were characterized using an ultraviolet-visible spectrophotometer (Thermo Fischer Scientific, USA) against a blank at ambient temperature over three distinct days. The nanoparticles synthesized by cyanobacterial strains were analyzed for particle size using DLS particle size analyzers (Malvern Panalytical Nano ZS®, UK). Samples exhibiting unique absorption spectra of nanoparticles, characterized by the absence of sedimentation and the presence of colloidal stability, were chosen. Four sealed glass vials containing 5 ml of supernatant containing nanoparticles were prepared. These vials were subjected to analysis for DLS and zeta potential measurement. DLS was performed at a scattering angle of 90º at a temperature of 25 ºC on various days (Fig. 3).

Scanning electron microscope analysis (SEM)

A scanning electron microscope (SEM) was employed to analyze the synthesized nanoparticles. The strain in the logarithmic phase was isolated from control cultures (following a two-week period) and inoculated with a silver nitrate or zinc acetate solution for 48 hours. Subsequent to inoculation with these solutions, the cells were washed twice with deionized water and subjected to centrifugation. The resulting pellet was fixed in a 2% glutaraldehyde solution prepared in BG-11 medium. The resulting mixture was stored at 4 °C overnight for fixation. Subsequently, the cells were washed with distilled water, and 60 µL of the cell suspension were applied to 12 mm electron microscope slides that had been previously coated with poly-L-lysine and maintained at room temperature for 20 seconds to enable cell adhesion. Dehydration was then carried out using solutions

of 40, 60, 80, and 100% ethanol. The sample was dried, and SEM analysis was conducted using a scanning electron microscope (Zeiss EVO 18, Germany).

Fourier transform infrared spectroscopy analysis (FTIR)

To characterize nanoparticle properties and chemical bonds, the centrifuged and dried nanoparticles were subjected to Fourier-transform infrared spectroscopy (FTIR) analysis. FTIR analysis was conducted using PerkinElmer's Spectrum 3™ FT-IR Spectrometer employing the KBr pellet method at a resolution of 2 cm^{-1}.

Antibacterial effects of NPs

Minimum inhibitory concentration (MIC) and MBC of NPs

The susceptibility of fish pathogens associated with various genera, including Aeromonas hydrophila (ATCC 7966), Edwardsiella tarda (ATCC 15947), Yersinia enterocolitica (ATCC 23715), and Pseudomonas putida (ATCC 23467), to the synthesized nanoparticles was assessed using standardized methodologies. The strains were procured from the Pasteur Institute in Tehran, Iran. The minimum inhibitory concentration (MIC) was established through the broth microdilution method. In summary, the fresh overnight culture of the tested microorganism was concentrated twofold for the preparation of Mueller Hinton Broth (MHB) cell suspension for bacterial strains to achieve concentrations of 106 CFU/ml and 103 cells/ml. For the assay, gradient concentrations of each synthesized nanoparticle were sequentially added to the prepared bacterial inocula. Following thorough mixing, the inoculated microplates were incubated at 37 ºC for 24 hours on a rotary shaker at 200 rpm, and subsequently, optical density was measured using a microplate reader (Bio-Rad Hercules, CA, USA) at 600 nm. The MIC was defined as the lowest concentration of nanoparticles that suppresses the substantial growth of microorganisms. To ascertain the minimum bactericidal concentration (MBC), 100 µl of a portion of the broth was extracted from each well, transferred to BHI medium, and incubated at 37°C overnight. Twenty milliliters of cultures exhibiting no turbidity were inoculated onto BHI agar and incubated at 37°C for 24 hours. The lowest concentration at which the incubated microorganisms were entirely eliminated (as determined by the absence of colonies on the plate) was defined as MBC. Gentamicin served as a positive antimicrobial control.

Agar well diffusion analysis

The antibacterial efficacy of the nanoparticles was assessed using the agar-well diffusion method. In this methodology, a bacterial inoculum comprising 1.5 × 108 CFU/ml of each reference pathogen culture was prepared. The suspensions were subcultured on MHB at 37 °C, and the mixture was evenly applied to the individual plates using a swab. Subsequently, wells (6 mm) were created in the MH agar plates using a sterile Pasteur pipette. Each well was filled with 20 µL of the various dilutions of nanoparticle solutions. Streptomycin served as a positive control, while dimethyl sulfoxide (DMSO) was employed as a negative control. Subsequently, the plates were stored at room temperature for 24 hours, followed by incubation at 37°C overnight. Lastly, the diameter of the bacterial growth inhibition zone was recorded, and the average values were calculated. The experiment was conducted with three replications.

Ultrastructural time-dependent nanoparticles and pathogen interaction

The interaction between the synthesized nanoparticles and the most susceptible bacterium, Yersinia enterocolitica, was investigated using transmission electron microscopy (TEM) (FEI Tecnai G2 Spirit Twin TEM instrument, USA) to compare its impact on the bacterial outer membrane with untreated controls. Alterations were observed in the cell membranes of Yersinia enterocolitica following several incubation phases. In summary, a bacterial colony was introduced to 5 falcon tubes containing 5 ml of MHB and agitated (150 rpm) at room temperature until the conclusion of the logarithmic phase. Doubled weights of the MIC of nanoparticles were meticulously weighed and directly added to 4 tubes containing cultured bacteria. The fifth tube did not receive nanoparticles and served as a control. All tubes were maintained under identical conditions but at varying time intervals (30, 60, 120, and 180 minutes). Subsequent to each specific incubation period, the bacterial pellets were centrifuged at 11,600 × g for 15 minutes and resuspended in 1 ml of phosphate buffered saline (PBS), followed by another centrifugation step and subsequent utilization for TEM analysis.

All samples were preserved in glutaraldehyde (5% in 0.1 M PBS) for 3 hours at 4°C. Additional fixation was performed using 1% osmium tetroxide for two hours at 4°C, followed by two washing cycles with PBS and progressive dehydration using serial dilutions of ethanol (76, 96, and 100%). Subsequently, the samples were immersed in a 1:1 mixture of glycidyl ether and propylene oxide for 45 minutes and then incubated overnight in a 3:1 mixture of glycidyl ether and propylene oxide. Sectioning was then performed using a steel knife with the aid of an ultramicrotome. Thin sections were stained twice with uranyl acetate and saturated lead citrate (pH: 7.4) and imaged.

Cytotoxicity assay

Fish cell lines and culture condition

The impact of synthesized nanoparticles on the viability of fish cell lines was assessed to evaluate their safety as therapeutic agents in vitro, adhering to the methodology outlined by **Ahmed et al. (Ahmed et al., 2020)**. Rainbow trout cell lines (RTG-2) were cultivated in tissue culture plates containing L-15 medium (Gibco) supplemented with antibiotics (Streptomycin 100 µg/ml and Penicillin 100 IU/ml) and 10% fetal bovine serum, maintained at 20°C for a duration of 24 hours. The approximate seeding density was 3×105 cells/cm2.

Cytotoxicity and cell viability

In vitro cytotoxicity assays of the synthesized nanoparticles were conducted to assess their impact on the viability of fish cell lines. Cell viability was evaluated after 24 and 48 hours of incubation with varying doses of nanoparticles. In summary, 100 µl containing approximately 1.5×105 cells were seeded into each well containing 1 ml of minimum essential medium (MEM, Gibco) and incubated at 20°C for 24 hours. Subsequent to forming a monolayer, all wells were inoculated with fresh medium containing varying concentrations of either ZnO or Ag nanoparticles (0–200 µg/ml), with the exception of the negative control wells, and incubated at 20 °C for 24 hours. The cytotoxicity of selected nanoparticle doses was assessed using a trypan blue exclusion assay **(Ahmed et al., 2020)**. Briefly, following incubation periods, the culture medium was decanted, and the cells were gently washed with phosphate-buffered saline to remove any residual nanoparticles. The cells were mixed (1:1) with 0.4% trypan blue for 60 seconds. The dye was fixed with 4% formalin for 10 minutes, and subsequently, the cells were washed three times with phosphate-buffered saline and examined under an inverted microscope. The number of dead cells (blue) was counted in relation to the number of live cells (unstained) per hundred cells. The percentage of viable cells per well was expressed as the mean ± standard error. The assay was conducted in triplicate, with three replicates of each well and one control well per assay.

Statistical analysis

The outcomes of the assays conducted on the samples were analyzed using SPSS software (SPSS package program, version 16.0, SPSS Inc., USA). Duncan's mean comparison test was employed to compare the mean values of the assays. The statistical significance of the differences between the means was examined at a $p< 0.05$ level.

RESULTS

Comparison of various synthesis methods

The results of the comparison of absorption spectra of silver and zinc nanoparticles biosynthesized by Neowestiellopsis persica through various methodologies are depicted in Figures 1 and 2, respectively. In the current investigation, both Ag and ZnO NPs were successfully synthesized through diverse methodologies, as verified by UV-Vis spectrophotometry. The maximum peak at 380 nm for NPs produced through the biomass boiling method was notably higher than other samples after the initial 12 hours ($p<0.05$).

The absorbance intensities of both NPs biosynthesized through the C-Phycocyanin and Extracellular Polysaccharides methods exhibited a significant increase over time ($p<0.05$), unequivocally indicating the enhanced formation of NPs. Taking into account these findings, the Ag and ZnO NPs synthesized through the biomass boiling method were chosen for subsequent stages.

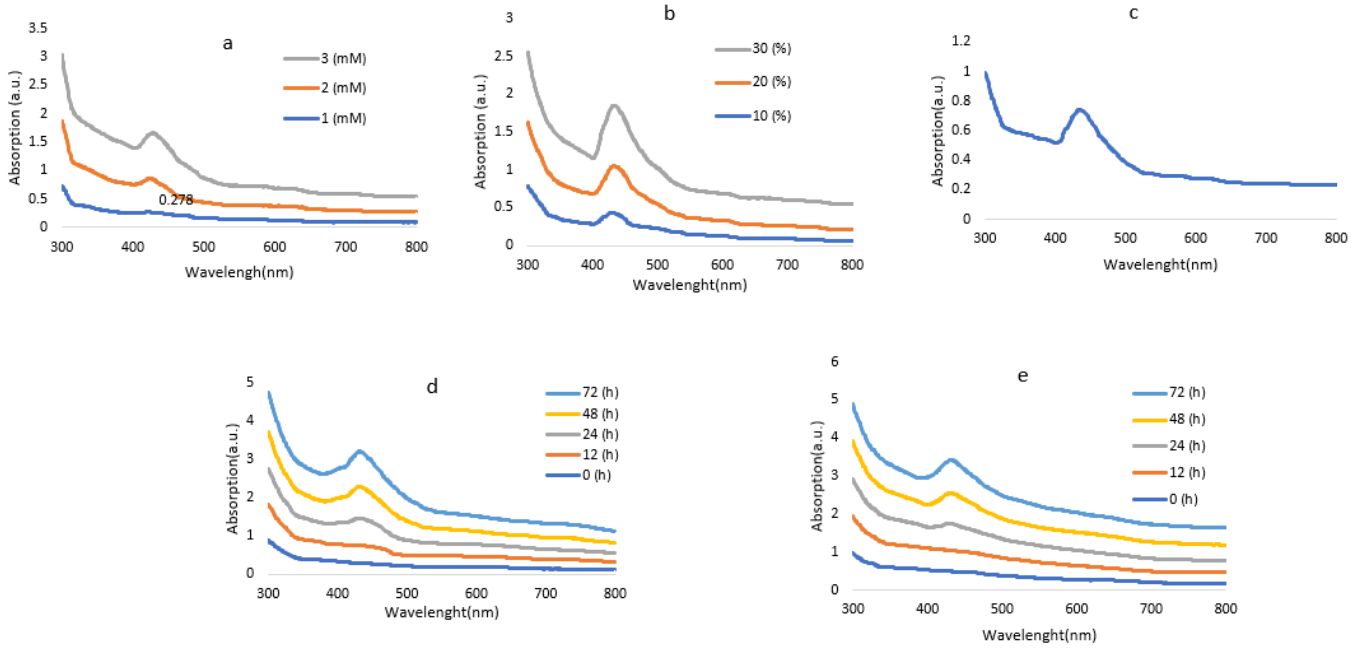

Figure 1 Comparison of absorption spectra of silver nanoparticles prepared through different methods**.** (a) Wet biomass (b) Supernatant (c) Boiling the biomass (d) C-Phycocyanin (e) Extracellular polysaccharides. Conditions: Varying concentrations of silver nitrate (10%, 20%, and 30%) and different time periods (0-72 hours).

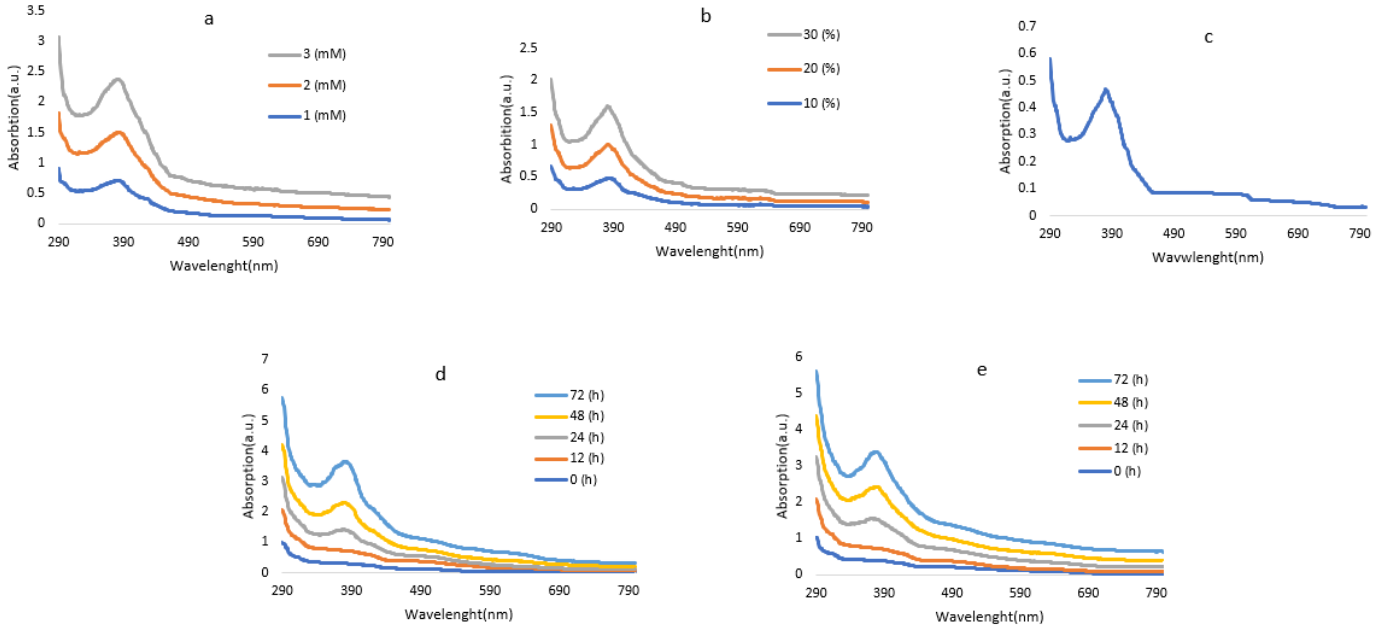

Figure 2 Comparison of absorption spectra of zinc oxide nanoparticles prepared through different methods. (a) Wet biomass (b) Supernatant (c) Boiling the biomass (d) C-Phycocyanin (e) Extracellular polysaccharides **Conditions:** Varying concentrations of zinc acetate (10%, 20%, and 30%) and different time periods (0-72 hours).

Characterization of NPs

The DLS results indicated that 41.2% and 45.5% of the Ag NP sizes were 78.82 nm and 91.28 nm, respectively, suggesting the existence of two distinct populations of Ag NPs. DLS analysis of the synthesized silver and zinc oxide nanoparticles revealed single absorption peaks for ZnO nanoparticles, indicative of a homogeneous population. The DLS demonstrated a pronounced absorption peak at 68.6 nm (80.1%) for ZnO nanoparticles (Figure. 1). Zeta potential analysis revealed substantial differences in the surface charge between the nanoparticles produced through various methods. Nanoparticles synthesized through the biomass boiling method exhibited a pronounced negative surface charge (-42.67±0.31 and -31.54±0.43 mV for Ag and ZnO NPs, respectively), whereas other synthesized nanoparticles displayed a surface charge closer to zero (-12.1 mV) or even positive.

Microscopic assay of NPs

SEM images depicting homogeneous spherical particles and agglomerations of silver and zinc oxide nanoparticles, respectively, are presented in Figure 3. The scanned Ag nanoparticles exhibited a diameter range of 43.12 nm, whereas ZnO NPs displayed a diameter of 78.74 nm at a magnification of 1 µm.

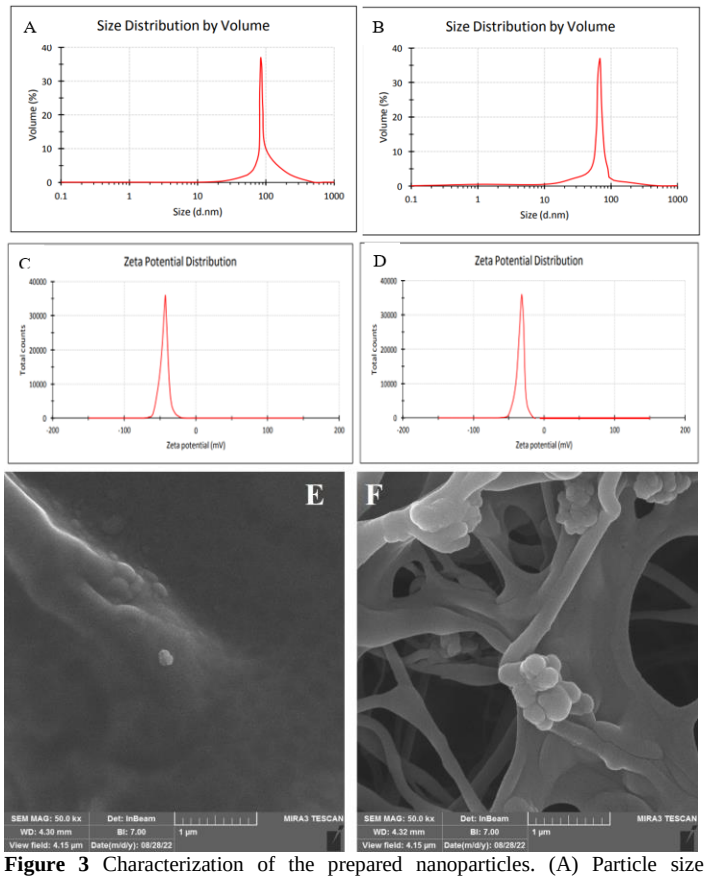

Figure 3 Characterization of the prepared nanoparticles. (A) Particle size distribution of silver nanoparticles (B) Particle size distribution of zinc oxide nanoparticles (C) Zeta potential distribution of silver nanoparticles (D) Zeta potential distribution of zinc oxide nanoparticles (E) Scanning electron microscopy (SEM) image of silver nanoparticles (F) Scanning electron microscopy (SEM) image of zinc oxide nanoparticles

FTIR analysis

The FT-IR spectra of silver and zinc oxide nanoparticles are depicted in Figures 4a and 4b, respectively. As depicted in Figure 4a, the first and second peaks correspond to the stretching vibration of the OH and CH bonds, which has exhibited inversion at 3405.38 and 2965 cm^{-1}.

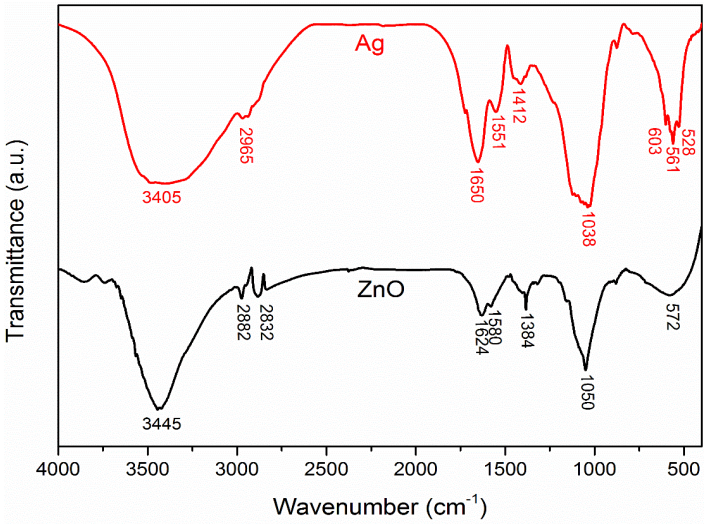

Figure 4 Fourier-transform infrared (FTIR) spectra of cyanobacterial-derived nanoparticles. (a) Silver nanoparticles (b) Zinc oxide nanoparticles

The peaks at 528.08 and 560.98 cm-1 were attributed to the stretching vibration of the silver lattice parameter. Lastly, the remaining peaks at 1650.07, 1038.48, 1412.72, and 1551.95 cm-1 are all associated with silver-forming materials (respectively related to aromatic ring stretching vibration, C-O group stretching vibration, and the bending of the CH2 and CH3 bonds) and can be attributed to the bacterial protein. Concerning the ZnO spectrum, the first peak at the wavenumber of 3445.13 cm-1 is inversely related to the stretching vibration of the OH bond, resulting from the presence of moisture within the system. The peaks at 2882.21 and 2832.98 cm-1 are attributed to the stretching vibration of the C-H bond. The peak at the wavenumber of 572.49 cm-1 is caused by the stretching vibration of the Zn-O bond. The peaks at 1050.85, 1384.42, and 1628.94 cm-1 are respectively associated with the stretching vibration of the C-O bond, the bending vibration of the CH2 bond, and the stretching vibration of the aromatic ring, which are related to zinc oxide constituents and can be attributed to the cyanobacterial proteins (Figure. 4).

MIC and MBC

The growth of all strains was entirely suppressed following incubation with synthesized Ag and ZnO nanoparticles (Tables 1). The absence of strain growth in MH agar and BHI corroborated the MIC test results. The turbidimetric method demonstrated that both Ag and ZnO NP suspensions exhibited substantial antibacterial effects against all tested strains in a species-specific and dose-dependent manner.

Table 1 Minimum inhibitory concentrations (MICs) and Minimum bactericidal concentrations (MBCs) (µg/ml) of the biosynthesized silver and zinc nanoparticles.

Pathogen	**Ag Biosynthesize methods**																	
	WB 1mM		WB 2mM		WB 3mM		Su10%		Su20%		Su30%		BB		C-P		EP	
	MIC	MBC	MIC	MBC	MIC	MBC	MIC	MBC	MIC	MBC	MIC	MBC	MIC	MBC	MIC	MBC	MIC	MBC
A. *hydrophila*	5	2.5	5	1.25	5	1.25	5	2.5	10	2.5	5	1.25	1.25	0.625	5	1.25	10	2.5
E. tarda	10	5	10	1.25	10	1.25	20	2.5	10	2.5	10	1.25	1.25	0.625	5	1.25	20	2.5
Y. enterocolitica	5	0.625	5	0.625	2.5	0.625	10	0.625	10	0.625	2.5	0.625	0.625	0.312	5	1.25	10	1.25
P. putida	40	2.5	10	2.5	5	1.25	20	2.5	10	2.5	5	2.5	1.25	1.25	5	2.5	20	5
Pathogen	**ZnO Biosynthesize methods**																	
	WB 1mM		WB 2mM		WB 3mM		Su10%		Su20%		Su30%		BB		C-P		EP	
	MIC	MBC	MIC	MBC	MIC	MBC	MIC	MBC	MIC	MBC	MIC	MBC	MIC	MBC	MIC	MBC	MIC	MBC
A. *hydrophila*	5	2.5	5	2.5	5	2.5	10	2.5	10	2.5	5	1.25	1.25	0.312	5	1.25	10	2.5
E. tarda	10	5	10	5	5	2.5	10	5	10	5	5	2.5	1.25	1.25	5	0.625	20	5
Y. enterocolitica	5	1.25	5	2.5	10	1.25	5	2.5	5	2.5	2.5	1.25	0.625	0.312	5	1.25	10	5
P. putida	10	10	5	2.5	2.5	1.25	10	5	10	5	5	2.5	1.25	0.625	5	1.25	10	1.25

WB: wet biomass, SU: supernatant, BB: Boiling the Biomass, CP: C-Phycocyanin and EP: Extracellular polysaccharides

The lowest MIC concentration of Ag NPs was observed against Yersinia enterocolitica at 0.625 mg/ml, whereas the highest MIC value was recorded against Pseudomonas putida and E. tarda at 20 mg/ml. The lowest MIC concentration of ZnO NPs was observed against Yersinia enterocolitica at 0.625 mg/ml, while the highest MIC value was recorded against Pseudomonas putida at 40 mg/ml. Nanoparticles synthesized through the biomass boiling method demonstrated significantly lower MIC values against the tested strains compared to other NPs ($p<0.01$).

The lowest concentration of the biosynthesized NPs via all methods that were capable of inhibiting bacterial growth on agar plates was recorded. Both Ag and ZnO NPs synthesized through the biomass boiling method exhibited a superior bactericidal effect compared to other NPs and all controls ($p<0.01$). The lowest MBC was determined against Yersinia enterocolitica at 0.315 mg/ml, indicating the highest sensitivity to both Ag and ZnO nanoparticles, while the highest MBC values were recorded at 5 mg/ml for Ag NPs against Edwardsiella tarda and at 10 mg/ml for ZnO NPs against Pseudomonas putida.

Antibacterial activity

There was no discernible difference in the antibacterial efficacy of zinc and silver nanoparticles synthesized using the boiling biomass technique ($p > 0.05$). The highest rate of growth suppression against selected strains was observed in nanoparticles synthesized through the boiling biomass method, while nanoparticles produced through other methods exhibited a lower rate of growth suppression ($p<0.05$).

Generally, biosynthesized silver nanoparticles produced using the boiling biomass method demonstrated a zone of inhibition for Aeromonsa hydrophila (17.2 ± 1.8mm), Edwardsiella tarda (18.2± 2.2 mm), Yersinia enterocolitica (17.9 ± 1.9 mm), and Pseudomonas putida (20.3 ± 1.7 mm). The zone of inhibition of zinc oxide nanoparticles for Aeromonsa hydrophila (20.1 ± 2.1 mm), Pseudomonas putida (19.8 ± 2.3 mm), and Yersinia enterocolitica (20.9 ± 1.8mm) was significantly high, while the zone of inhibition was observed to be lower for Edwardsiella tarda (11.3 ± 1.1mm).

Ultrastructural interaction between nanoparticles and *Yersinia enterocolitica*

Transmission electron microscopy images revealed spherical nanoparticles with uniform sizes and smooth surfaces. Experimental results indicated that the nanoparticles exhibited the greatest antimicrobial activity against Yersinia enterocolitica strains. Silver (Figure 5a) and zinc oxide (Figure 5d) nanoparticles were observed to adhere to the outer membrane of Yersinia enterocolitica. At higher magnifications, it was evident that the nanoparticles expanded the periplasmic space and caused diffuse swelling within the cytoplasm. Ultimately, silver (Figure 5b) and zinc (Figure 5e) nanoparticles disrupted the bacterial cell membrane, leading to complete cell rupture and the leakage of intracellular contents. Furthermore, smaller silver (Figure 5c) and zinc (Figure 5f) nanoparticles were observed within the bacterial cytoplasm (Figure 5).

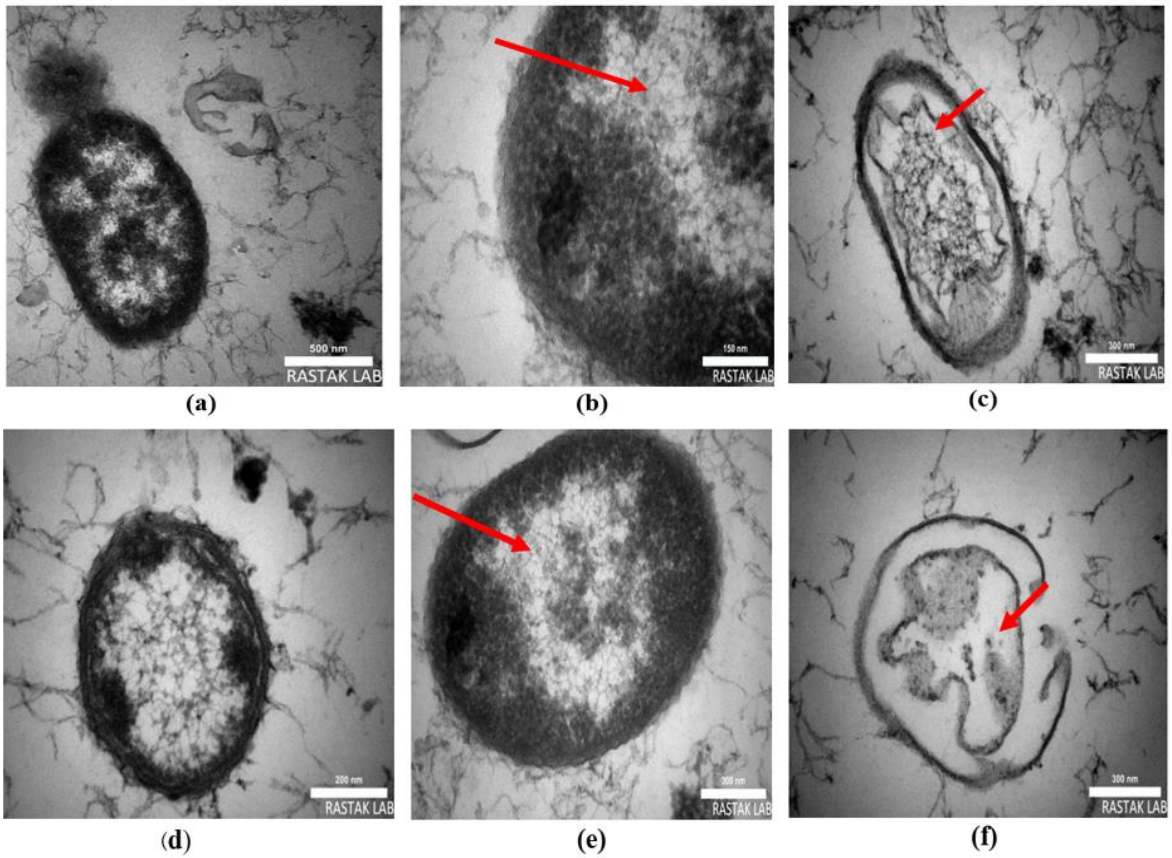

Figure 5 Transmission electron microscopy micrograph depicting the interaction between nanoparticles and Bacillus Yersinia enterocolitica. (a) Adherence of silver nanoparticles to the external membrane of the bacteria, (b) Enlargement of the periplasmic region (arrow), and (c) bacterial cell rupture and silver nanoparticles within the cytoplasm (arrow), (d) Clustering and adhesion of zinc nanoparticles to the outer membrane of Y. enterocolitica (e) Expansion of the periplasmic region (arrow), (f) zinc oxide nanoparticles within the cytoplasm (arrow), and cell disintegration.

Table 2 Viability of RTG-2 cells exposed to varying concentrations of both biogenic nanoparticles.

NPs concentrations (µg/ml)	Ag exposed cell survival (%)	ZnO exposed cell survival (%)
200	48.3 ± 2.1 (a)	83.1 ± 4.8 (a)
100	58.4 ± 4.3 (b)	84.32 ± 4.2 (b)
50	79.3 ± 9.3 (c)	60.4 ± 2.1 (c)
25	82.1 ± 10 (d)	72 ± 2.7 (d)
12.5	85 ± 10.4 (d)	76.2 ± 3 (d)
6.25	92.1 ± 11 (d)	81.45 ± 3.2 (e)
3.125	93.5 ± 11.6 (d)	84.32 ± 5.4 (e)
1.5625	96 ±12(d)	92.7 ± 9.8 (e)
0.78125	97.3 ± 12.1 (d)	94.1 ± 10 (e)
0.390625	100 ± 15 (d)	96.3 ± 11 (e)
0.195313	100 ± 13.3 (d)	99.2 ± 11.08 (e)
0	100 ± 15.1 (d)	100 ± 13.2 (e)

The values are expressed as Mean± SD. Different letters (a-e) in the same column indicate significant differences between ($p \leq 0.05$).

The cell viability following incubation with 25 µg/ml of silver nanoparticles and 6.25 µg/ml of zinc oxide nanoparticles, both synthesized using the boiling biomass method, exhibited no significant difference compared to untreated control cells. Statistical analysis revealed that as nanoparticle concentrations increased, cell viability decreased markedly ($p<0.05$) (Table 2). The lowest survival of RTG-2 cells was observed at 200 µg/ml concentrations of either silver or zinc oxide nanoparticles.

DISCUSSION

Aquaculture is currently one of the primary sources of sustenance for human populations, and the impact of various pathogens on it results in substantial losses (Sherif et al., 2021). Moreover, the growing resistance to antibiotics and their associated adverse effects on both humans and fish have prompted scientists to explore alternative antimicrobial agents with fewer side effects and greater efficacy (Kukułowicz et al., 2021). Meanwhile, metal oxide nanoparticles have been the focus of extensive research for their potential applications in diverse medical contexts, including fish health (Nasr-Eldahan et al., 2021). In this study, we investigated the antibacterial activity of silver and zinc oxide nanoparticles biosynthesized using the Iranian cyanobacterial strain, *Neowestiellopsis persica*, and compared the effects of different synthesis methods on their properties. The UV-Vis analysis of the produced silver and zinc oxide nanoparticles revealed absorbance peaks within the expected spectral range for these nanoparticles, confirming their successful synthesis through all methods. Similarly, Rashad et al. (2019), in their study on the antibacterial activity of biosynthesized silver nanoparticles using *Spirulina platensis* against oral pathogens, reported that the

formation of silver nanoparticles was confirmed using a UV-visible spectrophotometer with the surface plasmon resonance (SPR) at 425 nm.
The size distribution analysis of silver nanoparticles revealed two distinct populations of these nanoparticles; however, the majority of zinc oxide nanoparticles were concentrated within a single peak. Transmission electron microscopy images demonstrated that both types of nanoparticles adhered to the outer membrane of *Yersinia enterocolitica*. Our findings indicated that both nanoparticles exhibited significant antibacterial activity against all pathogens, which aligns with previous reports (Ghetas et al., 2022; Sarkar et al., 2022). It has been reported that, due to their small size, nanoparticles have a larger surface area in contact with the external environment, leading to a greater impact on the cell membrane. To the best of our knowledge, this is the first study to demonstrate the antimicrobial effects of silver and zinc oxide nanoparticles synthesized by *Neowestiellopsis persica* against fish pathogens. Our results revealed that biosynthesized silver and zinc oxide nanoparticles exhibited species-specific and dose-dependent antimicrobial efficacy. The findings demonstrated that silver nanoparticles (0.312 to 5 µg/ml) exhibited the maximum growth inhibitory effect against *Pseudomonas putida* and *Edwardsiella tarda*, followed by *Aeromonsa hydrophila* and *Yersinia enterocolitica*. Conversely, zinc oxide nanoparticles (0.625 to 5 µg/ml) showed the maximum inhibition zone against *Yersinia enterocolitica*, *Pseudomonas putida*, and *Aeromonsa hydrophila*, while the zone of inhibition was observed to be lower for *Edwardsiella tarda*. These findings are consistent with previous studies suggesting the antimicrobial effects of both silver and zinc nanoparticles (Ghetas et al., 2022; Shahzad Shirazi et al., 2022). In this research, the minimum inhibitory concentration (MIC) values of nanoparticles produced through different fabrication methods were significantly correlated with the concentration of silver nitrate and zinc acetate solutions. Additionally, a significant difference was observed between the MIC and minimum bactericidal concentration (MBC) values of nanoparticles synthesized using the boiling biomass method compared to other nanoparticles, regardless of the solutions' concentration.
We assessed the interaction between the nanoparticles and *Yersinia enterocolitica* strains at a structural level. Transmission electron microscopy revealed that nanoparticles larger than 15 nm were bound to the outer cell membrane, disrupting its function and integrity. Particles with a diameter of less than 7 nm were observed within the bacterial cells (Figure 5). These findings regarding the observation of nanoparticle aggregations within the cytoplasm are consistent with previous studies suggesting that smaller nanoparticles could pass through surface layer pores and interact directly with intracellular elements (Sirelkhatim et al., 2015). The antimicrobial effects of zinc and silver nanoparticles are not solely attributed to their penetration into the cells but also to various mechanisms such as the induction of oxidative stress and the production of oxygen free radicals, the disruption of cell membrane arrangement due to the attachment of the nanoparticles to the bacterial membrane, and their accumulation within the cytoplasm (Agarwal et al., 2018). Additionally, the electrostatic interaction between the bacterial surface and the nanoparticles, or zinc and silver ions, has been reported to contribute to the perforation of the bacterial cell wall. Soror et al. (Soror et al., 2022) and Shaalan et al. (2017) described similar observations, noting that the destruction of bacterial membranes by silver or zinc nanoparticles depends on their size and shape, which induces the formation of free radicals with potent antibacterial activity. The cytotoxicity assay demonstrated no difference between the lowest concentrations of both silver (25 µg/ml) and zinc oxide (6.25 µg/ml) nanoparticles and the control group, while cell viability decreased in a dose-dependent manner. In line with previous studies (Shaalan et al., 2017), silver nanoparticles exhibited fewer cytotoxic effects compared to zinc oxide nanoparticles. It has been reported that higher concentrations of silver and zinc oxide nanoparticles were genotoxic and cytotoxic to human and fish cell lines (Ahari et al., 2022; Rodriguez-Garraus et al., 2020; Singh, 2019).

CONCLUSION

Silver and zinc oxide nanoparticles were biosynthesized using *Neowestiellopsis persica* through various methods, which represent an environmentally friendly, cost-effective, and efficient process. The growth inhibition rate demonstrated that both nanoparticles synthesized in this research possess significant antibacterial activity against pathogenic strains. Consequently, biologically synthesized metal oxide nanoparticles could potentially be utilized in fish medicine for their effective antimicrobial capabilities, although further in vivo studies are still required to evaluate the antibacterial efficacy of these agents in living fish.

Abbreviation List

Zinc Oxide (ZnO NPs)
Silver Nanoparticles (AgNPs)
Scanning Electron Microscopy (SEM)
Fourier Transform Infrared Spectroscopy Analysis **(**FTIR)
Dynamic Light Scattering (DLS)
Transmission Electron Microscopy (TEM)
Minimum Inhibitory Concentration (MIC)
Mueller Hinton Broth (MHB)
Minimum Bactericidal Concentration (MBC)
Dimethyl Sulfoxide (DMSO)
Phosphate Buffered Saline (PBS)

Declaration of interest: Authors have no conflict of interest on this work
Acknowledgements: Not applicable
Funding: No funding was received for this work
Ethics approval: Not applicable
Availability of data and material: All data generated or analyzed during this study are available from the corresponding author on reasonable request.
Code availability: Not applicable
Informed consent: No human participants were involved in this study
Authors' contributions: OSJ: Conceptualization: writing—original draft preparation; EKh and R. K: software, validation, supervision; BN: formal analysis, methodology
All authors have read and agreed to the published version of the manuscript.

REFERENCES

Adeyemi, F. M., Ojo, O. O., Badejo, A. A., Oyedara, O. O., Olaitan, J. O., Adetunji, C. O. Akinde, S. B. (2022). Integrated poultry-fish farming system encourages multidrug-resistant gram-negative bacteria dissemination in pond environment and fishes. *Aquaculture*, *548*, 737558. https://doi.org/10.1016/j.aquaculture.2021.737558
Agarwal, H., Menon, S., Kumar, S. V., & Rajeshkumar, S. (2018). Mechanistic study on antibacterial action of zinc oxide nanoparticles synthesized using green route. *Chemico-biological interactions*, *286*, 60-70. https://doi.org/10.1016/j.cbi.2018.03.008
Ahari, H., Nowruzi, B., Anvar, A. A., & Porzani, S. J. (2022). The toxicity testing of cyanobacterial toxins In vivo and In vitro by mouse bioassay: A review. *Mini Reviews in Medicinal Chemistry*, *22*(8), 1131-1151. https://doi.org/10.2174/1389557521666211101162030
AHMADI, M. A., & NOUROUZI, B. (2008). A new report of n fixation by two species of cyanobacteria. *IRANIAN JOURNAL OF SCIENCE AND TECHNOLOGY TRANSACTION A- SCIENCE*, 32(A2),147-151.
Ahmed, F., Soliman, F. M., Adly, M. A., Soliman, H. A., El-Matbouli, M., & Saleh, M. (2020). In vitro assessment of the antimicrobial efficacy of chitosan nanoparticles against major fish pathogens and their cytotoxicity to fish cell lines. *Journal of Fish Diseases*, *43*(9), 1049-1063. https://doi.org/10.1111/jfd.13212
Anvar, S., Nowruzi, B., & Tala, M. (2021). Bioactive products of cyanobacteria and microalgae as valuable dietary and medicinal supplements. *Food Hygiene*, *11*(1 (41)), 99-118. https://doi.org/ 10.30495/JFH.2021.1925461.1310.
Anvar, S. A. A., Nowruzi, B., & Afshari, G. (2022). A Review of the Application of Nanoparticles Biosynthesized by Microalgae and Cyanobacteria in Medical and Veterinary Sciences. *Iranian Journal of Veterinary Medicine*, *17*(1), 1-18. http://dx.doi.org/10.32598/ijvm.17.1.1005309
Cepoi, L., Rudi, L., Chiriac, T., Valuta, A., Zinicovscaia, I., Duca, G., Pavlov, S. (2015). Biochemical changes in cyanobacteria during the synthesis of silver nanoparticles. *Canadian journal of microbiology*, *61*(1), 13-21. https://doi.org/10.1139/cjm-2014-0450
Chan, S. S., Low, S. S., Chew, K. W., Ling, T. C., Rinklebe, J., Juan, J. C., Show, P. L. (2022). Prospects and environmental sustainability of phyconanotechnology: A review on algae-mediated metal nanoparticles synthesis and mechanism. *Environmental research*, *212*, 113140. https://doi.org/10.1016/j.envres.2022.113140
Chen, J., Jayachandran, M., Bai, W., & Xu, B. (2022). A critical review on the health benefits of fish consumption and its bioactive constituents. *Food Chemistry*, *369*, 130874. https://doi.org/10.1016/j.foodchem.2021.130874
El Semary, N. A., & Bakir, E. M. (2022). Multidrug-resistant bacterial pathogens and public health: the antimicrobial effect of cyanobacterial-biosynthesized silver nanoparticles. *Antibiotics*, *11*(8), 1003. https://doi.org/10.3390/antibiotics11081003
Franco, D., Calabrese, G., Guglielmino, S. P. P., & Conoci, S. (2022). Metal-based nanoparticles: Antibacterial mechanisms and biomedical application. *Microorganisms*, *10*(9), 1778. https://doi.org/10.3390/microorganisms10091778
Fritz, M., Körsten, S., Chen, X., Yang, G., Lv, Y., Liu, M., Fischer, C. B. (2022). High-resolution particle size and shape analysis of the first Samarium nanoparticles biosynthesized from aqueous solutions via cyanobacteria Anabaena cylindrica. *NanoImpact*, *26*, 100398. https://doi.org/10.1016/j.impact.2022.100398
Ghetas, H. A., Abdel-Razek, N., Shakweer, M. S., Abotaleb, M. M., Paray, B. A., Ali, S., Khalil, R. H. (2022). Antimicrobial activity of chemically and biologically synthesized silver nanoparticles against some fish pathogens. *Saudi Journal of Biological Sciences*, *29*(3), 1298-1305. https://doi.org/10.1016/j.sjbs.2021.11.015
Golizadeh, Z., Nowruzi, B., & Falsafi, S. (2022). Study of antimicrobial activity of biosynthesized nanoparticles via two different methods by freshwater cyanobacteria Nostoc sp. *Biological Journal of Microorganism*, 12(46),51-68. https://doi.org/10.22108/bjm.2022.133646.1470
Guiry, M., & Guiry, G. (2020). AlgaeBase. World-wide electronic publication, National University of Ireland. Galway, Ireland. In.

Hamida, R. S., Ali, M. A., Redhwan, A., & Bin-Meferij, M. M. (2020). Cyanobacteria–a promising platform in green nanotechnology: a review on nanoparticles fabrication and their prospective applications. *International journal of nanomedicine*, *15*, 6033.
Ifijen, I. H., Maliki, M., & Anegbe, B. (2022). Synthesis, Photocatalytic Degradation and Antibacterial Properties of Selenium or Silver Doped Zinc Oxide Nanoparticles: A Detailed Review. *OpenNano*, 100082. https://doi.org/10.1016/j.onano.2022.100082
Jochum, M., Moncayo, L. P., & Jo, Y.-K. (2018). Microalgal cultivation for biofertilization in rice plants using a vertical semi-closed airlift photobioreactor. *PLoS One*, *13*(9), e0203456. https://doi.org/10.1371/journal.pone.0203456
Kabirnataj, S., Nematzadeh, G. A., Talebi, A. F., Tabatabaei, M., & Singh, P. (2018). Neowestiellopsis gen. nov, a new genus of true branched cyanobacteria with the description of Neowestiellopsis persica sp. nov. and Neowestiellopsis bilateralis sp. nov., isolated from Iran. *Plant Systematics and Evolution*, *304*(4), 501-510. https://doi.org/10.1007/s00606-017-1488-6
Krešić, G., Dujmić, E., Lončarić, D., Zrnčić, S., Liović, N., & Pleadin, J. (2022). Fish Consumption: Influence of Knowledge, Product Information, and Satisfaction with Product Attributes. *Nutrients*, *14*(13), 2691. https://doi.org/10.3390/nu14132691
Kukułowicz, A., Steinka, I., & Siwek, A. (2021). Presence of Antibiotic-Resistant Staphylococcus aureus in Fish and Seafood Originating from Points of Sale in the Tri-City Area (Poland). *Journal of Food Protection*, *84*(11), 1911-1914. https://doi.org/10.4315/JFP-21-115
Liu, L., Jokela, J., Wahlsten, M., Nowruzi, B., Permi, P., Zhang, Y. Z., Sivonen, K. (2014). Nostosins, trypsin inhibitors isolated from the terrestrial cyanobacterium Nostoc sp. strain FSN. *Journal of natural products*, *77*(8), 1784-1790. https://doi.org/10.1021/np500106w
Mathew, S., & Radhakrishnan, E. (2022). Health and Safety Issues of Nanotechnology in Food Applications. In *Nano-Innovations in Food Packaging* (pp. 247-276): Apple Academic Press.
Mutoti, M., Gumbo, J., & Jideani, A. I. O. (2022). Occurrence of cyanobacteria in water used for food production: A review. *Physics and Chemistry of the Earth, Parts A/B/C*, *125*, 103101. https://doi.org/10.1016/j.pce.2021.103101
Nasr-Eldahan, S., Nabil-Adam, A., Shreadah, M. A., Maher, A. M., & El-Sayed Ali, T. (2021). A review article on nanotechnology in aquaculture sustainability as a novel tool in fish disease control. *Aquaculture International*, *29*(4), 1459-1480. https://doi.org/10.1007/s10499-021-00677-7
Nowruzi, B. (2022). Cyanobacteria Natural Products as Sources for Future Directions in Antibiotic Drug Discovery. Cyanobacteria - Recent Advances and New Perspectives. http://doi.org/ 10.5772/intechopen.106364
Okeke, E. S., Chukwudozie, K. I., Nyaruaba, R., Ita, R. E., Oladipo, A., Ejeromedoghene, O., . . . Okoye, C. O. (2022). Antibiotic resistance in aquaculture and aquatic organisms: a review of current nanotechnology applications for sustainable management. *Environmental Science and Pollution Research*, 1-34. https://doi.org/10.1007/s11356-022-22319-y
Patel, V., Berthold, D., Puranik, P., & Gantar, M. (2015). Screening of cyanobacteria and microalgae for their ability to synthesize silver nanoparticles with antibacterial activity. *Biotechnology Reports*, *5*, 112-119. https://doi.org/10.1016/j.btre.2014.12.001
Peng, Y., Lai, X., Wang, P., Long, W., Zhai, F., Hu, S., . . . Yu, Z. (2022). The isolation of a novel Streptomyces termitum and identification its active substance against fish pathogens. *Reproduction and Breeding*, *2*(3), 95-105. https://doi.org/10.1016/j.repbre.2022.07.002
Ranjitha, S., Aroulmoji, V., Selvankumar, T., Sudhakar, C., & Hariharan, V. (2020). Synthesis and development of novel sensitizer from spirulina pigment with silver doped TiO2 nano particles for bio-sensitized solar cells. *Biomass and Bioenergy*, *141*, 105733. https://doi.org/10.1016/j.biombioe.2020.105733
Rashad, S., A El-Chaghaby, G., & A Elchaghaby, M. (2019). Antibacterial activity of silver nanoparticles biosynthesized using Spirulina platensis microalgae extract against oral pathogens. *Egyptian Journal of Aquatic Biology and Fisheries*, *23*(5 (Special Issue)), 261-266. https://dx.doi.org/10.21608/ejabf.2019.65907
Rodriguez-Garraus, A., Azqueta, A., Vettorazzi, A., & Lopez de Cerain, A. (2020). Genotoxicity of silver nanoparticles. *Nanomaterials*, *10*(2), 251. https://doi.org/10.3390/nano10020251
Sabzevari, O., Khajerahimi, A., Kazempoor, R., & Nowruzi, B. (2022). A review of the antimicrobial and toxic properties of nanoparticles as a new alternative in the control of aquatic diseases. *Sustainable Aquaculture and Health Management Journal*, *8*(1), 78-102. http://dx.doi.org/10.52547/ijaah.8.1.78
Sarkar, D. J., Mohanty, D., Raut, S. S., & Kumar Das, B. (2022). Antibacterial properties and in silico modeling perspective of nano ZnO transported oxytetracycline-Zn2+ complex [ZnOTc]+ against oxytetracycline-resistant Aeromonas hydrophila. *The Journal of Antibiotics*, *75*(11), 635-649. https://doi.org/10.1038/s41429-022-00564-0
Shaalan, M. I., El-Mahdy, M. M., Theiner, S., El-Matbouli, M., & Saleh, M. (2017). In vitro assessment of the antimicrobial activity of silver and zinc oxide nanoparticles against fish pathogens. *Acta Veterinaria Scandinavica*, *59*(1), 1-11. https://doi.org/10.1186/s13028-017-0317-9
Shahzad Shirazi, M., Moridi Farimani, M., Foroumadi, A., Ghanemi, K., Benaglia, M., & Makvandi, P. (2022). Bioengineered synthesis of phytochemical-adorned green silver oxide (Ag2O) nanoparticles via Mentha pulegium and Ficus carica extracts with high antioxidant, antibacterial, and antifungal activities. *Scientific reports*, *12*(1), 1-15. https://doi.org/10.1038/s41598-022-26021-4
Sherif, A. H., Gouda, M., Darwish, S., & Abdelmohsin, A. (2021). Prevalence of antibiotic-resistant bacteria in freshwater fish farms. *Aquaculture Research*, *52*(5), 2036-2047. https://doi.org/10.1111/are.15052
Singh, S. (2019). Zinc oxide nanoparticles impacts: Cytotoxicity, genotoxicity, developmental toxicity, and neurotoxicity. *Toxicology mechanisms and methods*, *29*(4), 300-311. https://doi.org/10.1080/15376516.2018.1553221
Sirelkhatim, A., Mahmud, S., Seeni, A., Kaus, N. H. M., Ann, L. C., Bakhori, S. K. M., Mohamad, D. (2015). Review on zinc oxide nanoparticles: antibacterial activity and toxicity mechanism. *Nano-micro letters*, *7*(3), 219-242. https://doi.org/10.1007/s40820-015-0040-x
Sivaraman, G., Vijayan, A., Rajan, V., Elangovan, R., Prendivillie, A., & Bachmann, T. (2022). Impact of antimicrobial use and antibiotic resistant pathogens in aquatic products-An Indian perspective. *Indian J Anim Health*, *61*(1), 14-22. https://doi.org/10.36062/ijah.2022.14821
Soror, A.-F. S., Ahmed, M. W., Hassan, A. E., Alharbi, M., Alsubhi, N. H., Al-Quwaie, D. A., Qahl, S. H. (2022). Evaluation of Green Silver Nanoparticles Fabricated by Spirulina platensis Phycocyanin as Anticancer and Antimicrobial Agents. *Life*, *12*(10), 1493. https://doi.org/10.3390/life12101493
Testerman, T., Beka, L., McClure, E. A., Reichley, S. R., King, S., Welch, T. J., & Graf, J. (2022). Detecting Flavobacterial Fish Pathogens in the Environment via High-Throughput Community Analysis. *Applied and environmental microbiology*, *88*(2), e02092-02021. https://doi.org/10.1128/AEM.02092-21
Tsikourkitoudi, V., Henriques-Normark, B., & Sotiriou, G. A. (2022). Inorganic nanoparticle engineering against bacterial infections. *Current Opinion in Chemical Engineering*, *38*, 100872. https://doi.org/10.1016/j.coche.2022.100872
Zhang, W., Zhao, J., Ma, Y., Li, J., & Chen, X. (2022). The effective components of herbal medicines used for prevention and control of fish diseases. *Fish & Shellfish Immunology*. 126,73-83. https://doi.org/10.1016/j.fsi.2022.05.036